Heliyon 6 (2020) e04883

Contents lists available at ScienceDirect

Heliyon

journal homepage: www.cell.com/heliyon

Research article

A comparative study of the physical and chemical properties of pelletized HKUST-1, ZIF-8, ZIF-67 and UiO-66 powders

Eleni Tsalaporta [a,b,*], J.M. Don MacElroy [a]

[a] University College Dublin, School of Chemical and Bioprocess Engineering, Belfield, Dublin, 4, Ireland
[b] University College Cork, Discipline of Process and Chemical Engineering, College Road, Cork, Ireland

ARTICLE INFO

Keywords:
Materials science
Chemical engineering
UiO 66
ZIF 67
HKUST 1
MOFs
ZIF 8
Pelletization

ABSTRACT

The physical and chemical properties of four metal organic frameworks were examined before and after the pelletization process with pressure (tablet) and binders (pellet) for their possible use in industrial or other commercial processes. Due to the uniqueness of their crystal structure, each MOF behaved differently under the same treatment. ZIF-8 proved to be very robust in the presence of binding materials (pellet) as well as after the application of pressure (tablet). The presence of water resulted in the reversible partial loss of their crystalline morphology in the case of HKUST-1 and UiO-66 (pellet). The crystal structure of ZIF-67 was irreversibly lost in the case of the pellet but it was well maintained under pressure (tablet).

1. Introduction

Metal Organic Frameworks (MOFs) are newly developed ultra-high surface area microporous materials with multiple applications. They are synthesized from metal oxide clusters and organic ligands and as a result there are numerous potential MOFs with distinguishable properties that could be produced simply by changing the ligands or the linkers [1, 2, 3, 4, 5, 6, 7, 8]. The uniqueness of the crystal structure and properties of each MOF do not allow generalization of their behaviour when subjected to a range of environmental factors and for this reason, no reliable conclusions can be made unless each MOF is examined separately.

Due to their extensive surface areas, several MOFs have been examined and found to be ideal for catalysis, gas separations and storage. More specifically, many researchers have proposed MOFs to be used as adsorbents for the capture of methane [9], CO_2 in the presence or absence of water [10, 11, 12, 13, 14, 15, 16, 17, 18, 19], or other gas separations such as hydrogen and nitric oxide [20] and these are only a few examples in the extended list of possible uses of MOFs. However, despite their significant potential, MOFs have not been employed in industrial applications yet. Their availability at commercial scale is limited and they are only obtainable in powder form. Most of the applied industrial processes such as heterogeneous catalytic reaction systems or fluid separation processes (e.g. Pressure/Vacuum Swing Adsorption (PSA/VPSA)) require pellet shaped materials.

The production of pellets and the effects of this process on the properties of the MOFs has started to be examined only recently. Peterson et al. [21] have examined the effects of pressure on HKUST-1 and UiO-66, showing that HKUST-1 maintained its properties while UiO-66 lost octane loading. They also examined the effect of pelletization pressure on the physical and chemical properties of HKUST-1 and UiO-66, indicating that both MOFs are suitable for tablet preparation, although there is some degradation in porosity. In another study, MIL-53(Al) lost 32% of its N_2 adsorption capacity when pelletized with a polyvinyl alcohol binder [22]. O'Neill et al. [23] reversed the process and created HKUST-1 pellets by attaching HKUST-1 to the surface of polyacrylamide (PAM) beads instead of making pellets from HKUST-1 powder. In this case, the N_2 uptake and the surface area of the HKUST-1- PAM beads were significantly decreased (up to 80%) compared to the properties of the original powder.

More recently, Delgado et al. [24] studied the agglomeration of HKUST-1 and ZIF-8 with polyvinylalcohol (PVA). The obtained extrudates showed a low reduction of surface area in comparison to the powders, with a potentially good performance in separation processes. Similarly, Edubilly and Gumma [25] have used the same binder (polyvinylalcohol) in order to investigate the agglomeration of UiO-66, with the agglomerates maintaining approximately 85% of the CO_2 adsorption

* Corresponding author.
E-mail address: eleni.tsalaporta@ucc.ie (E. Tsalaporta).

https://doi.org/10.1016/j.heliyon.2020.e04883
Received 3 April 2018; Received in revised form 26 February 2020; Accepted 7 September 2020

capacity of the powder. Lee et al. [26] have used a different technique for the shaping of UiO-66. This technique is the calcium alginate technique, originated from molecular gastronomy and biology. While this method is promising for the shaping of water-stable MOFs, such as UiO-66, in very small quantities, scaling up molecular based techniques can be very difficult.

In this work, a different pelletization method was examined and evaluated, as suggested by Tsalaporta et al. [27]. Four commercial MOFs (ZIF-8, ZIF-67, HKUST-1 and UiO-66) were pelletized with a binder (methylcellulose) and a cement (bentonite) and compared to pressurized powder (tablets) of the same materials, with a view to their subsequent use in industrial scale fluid treatment or separation processes. More specifically, the use of these pellet shaped MOFs in a Pressure Swing Adsorption process for CO_2 capture was examined and will be presented in a separate article.

2. Material and methods

2.1. Materials

HKUST-1, ZIF-8 and ZIF-67 were purchased from MOF Technologies (Belfast, UK) and UiO-66 was purchased from STREM Chemicals (Massachusetts, US).

2.2. Preparation of pellets

Methylcellulose and bentonite (Sigma Aldrich) were used for the formation of small cylindrical pellets (nominal diameter: 1.7mm, length: 4mm), as suggested by Tsalaporta et al. [27]. Methylcellulose was used as binder and bentonite was used as cement in order to create a homogeneous plastic and elastic paste with a view to maintaining the crystal structure of the MOFs. The optimised mass ratio of each paste was: 1 gr of MOF, 2 gr of deionized water, 0.15 gr of methylcellulose and 0.15 gr of bentonite. Different mass ratios were examined, however the produced pellets were lacking in hardness, therefore they were not suitable for the purposes of handling in an industrial setting. The suggested mass ratios of bentonite and methylcellulose were the minimum recommended mass ratios in order to ensure that the hardness of the pellets was equivalent to zeolite 13x pellets (70–80 on the Rockwell B hardness scale), and to prevent the creation and transfer of dust during agitation in a typical industrial process. All the powders were added in a beaker and were mixed. The water was added last and the contents of the shaker were mixed for 10 min until a paste was formed. The paste was introduced into a Makin's clay extruder and extracted in lines (diameter 1.7 mm). The lines were cut into 4mm cylindrical beads (pellets) and left to dry at room temperature for 24 h. In the cases where the MOF structure was degraded after the pelletization process, the pellets were regenerated with ethanol as suggested by Mathivathani et al. [28]. More specifically 100gr of pellets were mixed with 2 L of ethanol and stirred at room temperature from 24 to 96 h.

2.3. Preparation of tablets

Agglomerates were prepared using a hand pellet press. 1 gr powder of each MOF and 0.2 ml of ethanol were gently mixed, introduced into a 2 cm die and pressed at 100 bar for 1 min, in order to ensure having a robust tablet (optimised process). Ethanol was added to the powder in order to protect the crystal structure of the MOFs. In the case of ZIF-8 and UiO-66, the agglomerates were well shaped, forming a strong tablet (dimensions: 2 cm diameter/3 mm thickness). However, in the case of HKUST-1 and ZIF-67, the tablets were fragile and there was powder left in the die in both cases, indicating that the pressure was not sufficient. The tablets were only prepared for the comparison of their surface areas with the surface area of the extruded pellets, therefore the presented results are for illustrative purposes only.

2.4. SEM

Samples were mounted on stubs using double-sided carbon tape, and sputter coated with Gold, using an Emitech K575X Sputter Coating Unit, to prevent surface charging by the electron beam. Samples were then examined using a FEI Quanta 3D FEG DualBeam (FEI Ltd, Hillsboro, USA) at 5KV using 5.9 pA.

2.5. Nitrogen isotherms – surface area - porosity

Nitrogen porosimetry measurements were conducted using a Quantachrome Analyzer. All the samples were outgassed at 150 °C for 24 h. The BET method was used for measuring the surface area. The pore size distribution was calculated with non-local density functional theory (NLDFT) using a slit pore carbon kernel. The micropore volume was calculated using the Dubinin-Radushkevitch (DR) method and the total volume was measured at a relative pressure, P/P_o, of 0.99.

2.6. XRD

X-ray diffraction (PXRD) measurements were taken using a KRISTALLOFLEX X-ray Generator K760-A21. All the samples were scanned at 30mA and 40kV using CuKα radiation. The 2θ range was from 5^o to 40^o with a step size of 0.02^o. In order to minimize the background scattering, zero background discs were used. The analysis of the results were processed by the software Traces.

2.7. Hardness test

Hardness tests were conducted with a manual pellet hardness tester KAHL. The hardness was measured in kg/mm^2 and was converted to Rockwell B hardness scale.

3. Results and discussion

3.1. Characterization of ZIF-8

Table 1 summarizes all the samples of ZIF-8. Images of the powder, tablet and pellet are presented in Figure 1 while scanning electron microscope (SEM) images are presented in Figure 2 (a: powder, b: tablet, c: pellet). The micron-sized octahedral crystallites of the powder have maintained their structure and shape after the pelletization process. This fact is further supported by the XRD curves (Figure 3). The presence of two additional components, a binder and a cement, did not destroy the crystal structure of ZIF-8 but did cause a minor structural collapse and a displacement of the crystal peaks. The hardness of the pellets was measured as 71 on the Rockwell B hardness scale, which is comparable to 78 of commercial zeolite 13X pellets, measured for the purposes of this paper [33].

Nitrogen isotherms were measured in order to examine whether surface area and pore size were affected by the pelletization process (Figure 4). For comparative purposes, tablets of ZIF-8 powder were prepared in a hand pellet press and compared to the initial powder and the extruded pellet shaped material. Table 1 summarizes the BET surface area and the pore volume of the three samples. The decrease in the pore volume of the pellet shaped MOF was primarily due to the binding materials. Based on the proportions of ZIF-8, binder and cement, the actual decrease in the volume was approximately 7% per gram of ZIF-8.

3.2. Characterization of ZIF-67

A summary of ZIF-67 samples is presented in Table 2 and images of the powder and pellets are presented in Figure 5. Scanning electron microscope (SEM) images are presented in Figure 6 (a: powder, b: tablet, c: pellet). Unlike ZIF-8, the structure of ZIF-67 was irreversibly destroyed in the presence of the three components, water, binder and cement. Attempts to regenerate the degraded structure with ethanol were

Table 1. Surface and pore properties of ZIF-8.

ZIF-8 Sample	BET surface area m^2/g	Pore volume cc/g	Pore diameter Å
ZIF-8 powder	2047.1	0.460	15.6
ZIF-8 tablet	1681.5	0.458	15.3
ZIF-8 pellet	1471.5	0.333	14.7

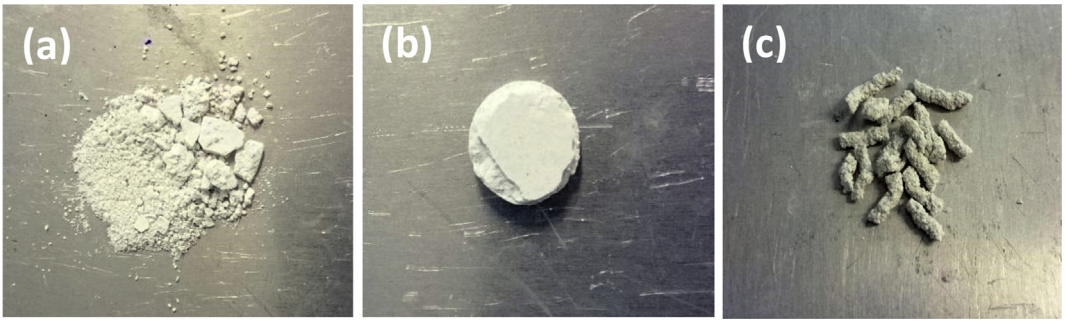

Figure 1. ZIF-8 samples: (a) powder, (b) tablet and (c) pellet.

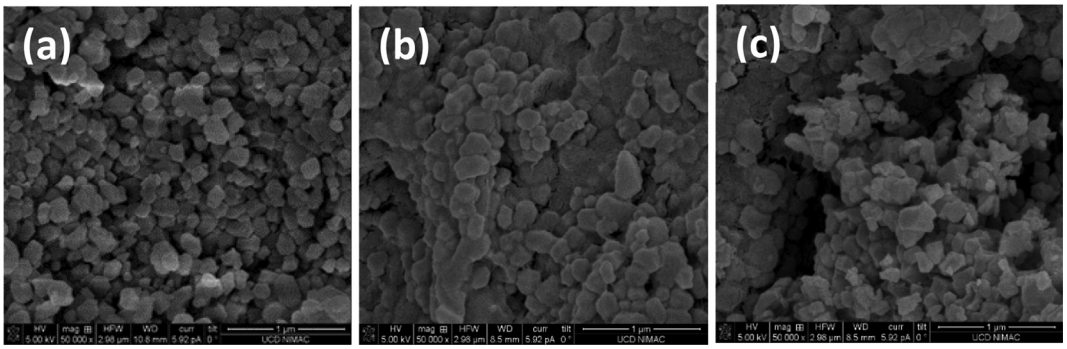

Figure 2. SEM images for ZIF-8 samples: (a) powder, (b) tablet and (c) pellet.

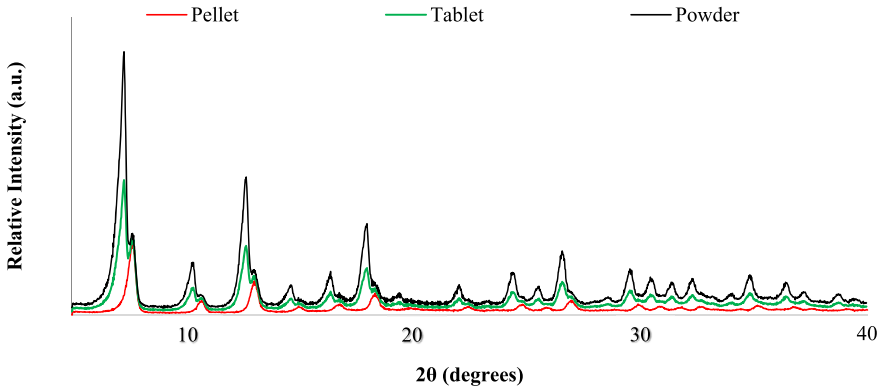

Figure 3. Comparison of the XRD patterns – ZIF-8.

unsuccessful. More specifically, less than 35% of the initial surface area was maintained in the pellet shaped material before and after ethanol treatment. The decrease in the pore volume due to the binding materials was 49% per gram of ZIF-67. The N_2 isotherms of the powder and the pellet are presented in Figure 7. However, as cited in Table 2, the applied pressure in the case of the tablet has only caused a minor structural collapse by maintaining 75% of the initial state.

The XRD patterns were in line with the surface area analysis, showing a minor structural collapse in the case of the tablet and a very serious one in the case of the pellet (Figure 8). Similarly, the SEM images of the powder and the tablet indicate well shaped spherical crystals with interstitial macropores while in the case of the pellet, the pores are filled and the crystals have lost their shape. Finally, the hardness of the pellets was similar to ZIF-8 pellets, at 69 of Rockwell B hardness scale [33].

3.3. Characterization of HKUST 1

HKUST 1 powder, tablet and pellet images are shown in Figure 9, with the hardness of the pellets being 70 Rockwell B [33]. Unlike ZIF-8, HKUST-1 powder proved to be very sensitive to any pelletization

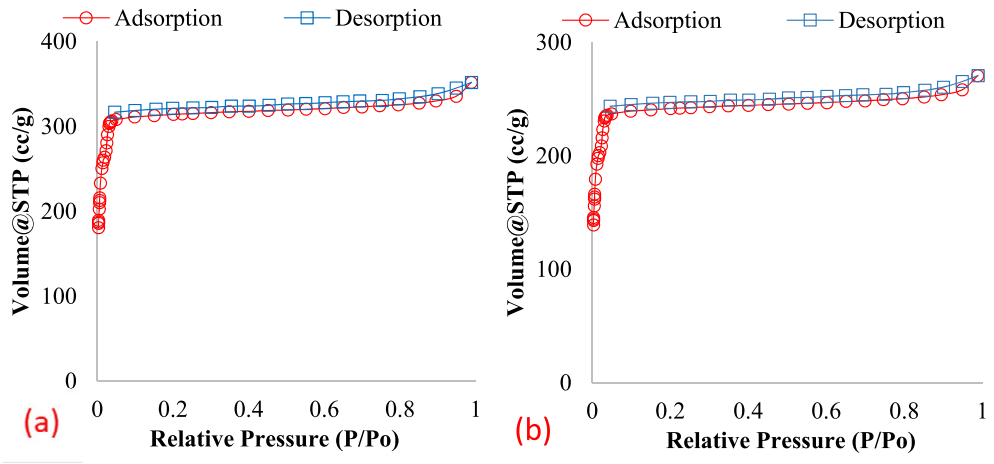

Figure 4. (a) N_2 isotherm for ZIF-8 powder (b) N_2 isotherm for ZIF-8 pellet.

Table 2. Surface and pore properties of ZIF-67.

ZIF-67 Sample	BET surface area m^2/g	Pore volume cc/g	Pore diameter Å
ZIF-67 powder	1789.6	0.660	16.3
ZIF-67 tablet	1334.9	0.495	16.2
ZIF-67 pellet	464.4	0.341	35.4

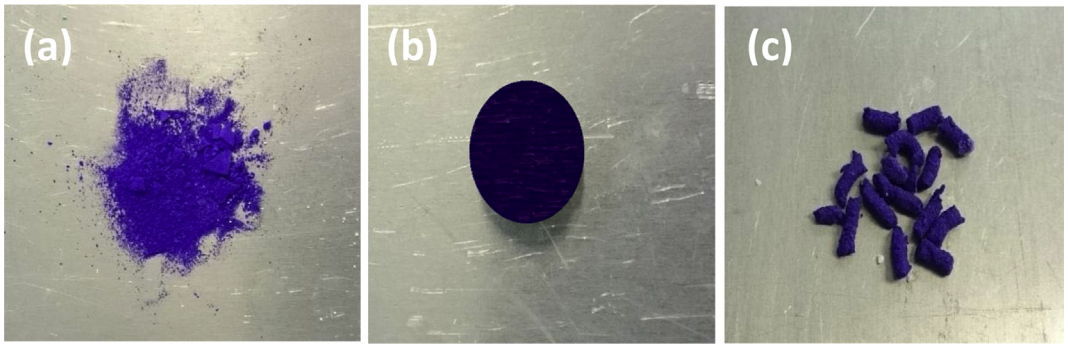

Figure 5. ZIF 67 samples: (a) powder, (b) tablet and (c) pellet.

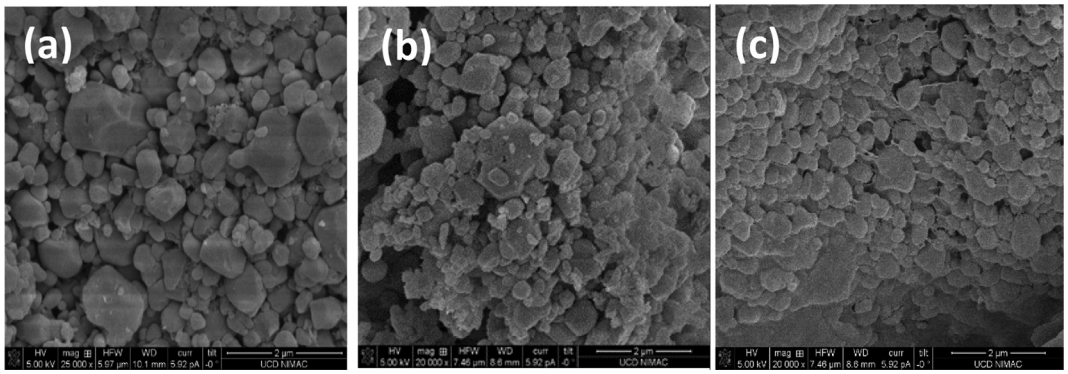

Figure 6. SEM images for ZIF-67 samples: (a) powder, (b) tablet and (c) pellet.

process (pressed or extruded). The BET surface area and pore volume measurements (see Table 3) indicated a dramatic loss in the surface area of both tablets and pellets. Furthermore, evidence for the collapse of the porous network of the pellets was provided by the lower signal intensity of the XRD patterns (Figure 10) indicating the deterioration of the crystal structure of the pellets compared to the high signal intensity of the powder. The degradation in the case of the tablet was due to the applied pressure and was irreversible while in the case of the pellets, it was subject to the water exposure (hydrolysis) and could be easily reversed, as reported by Majano et al. [29].

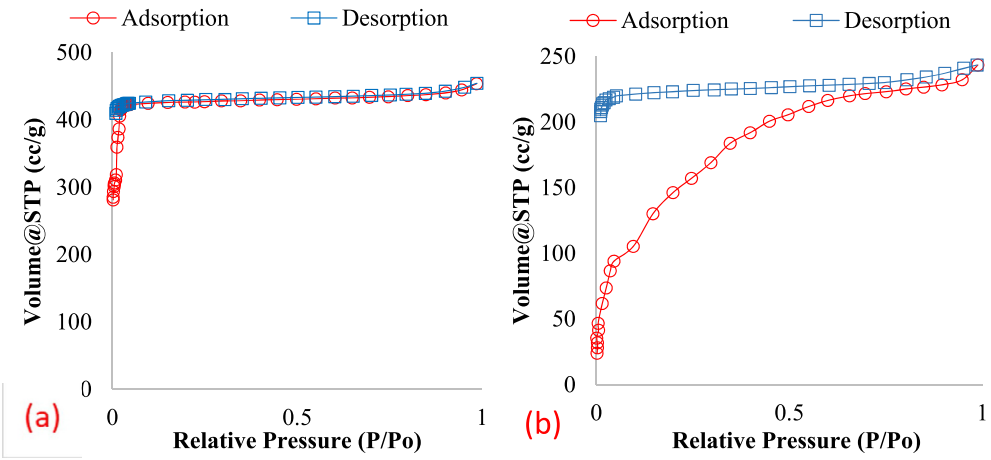

Figure 7. (a) N_2 isotherm for ZIF-67 powder (b) N_2 isotherm for ZIF-67 pellet.

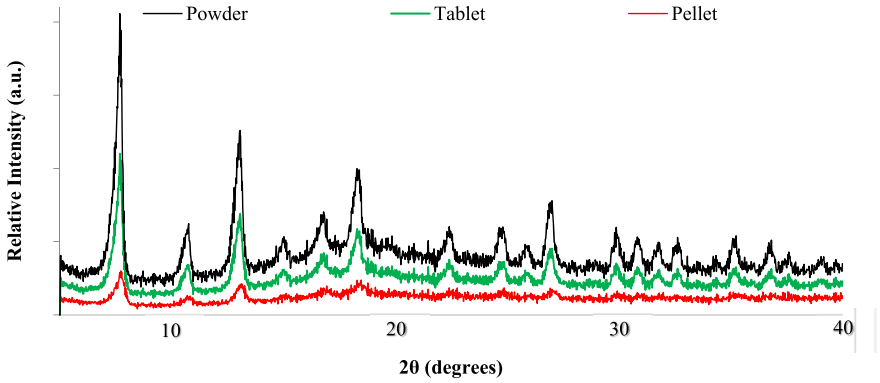

Figure 8. Comparison of the XRD patterns – ZIF-67.

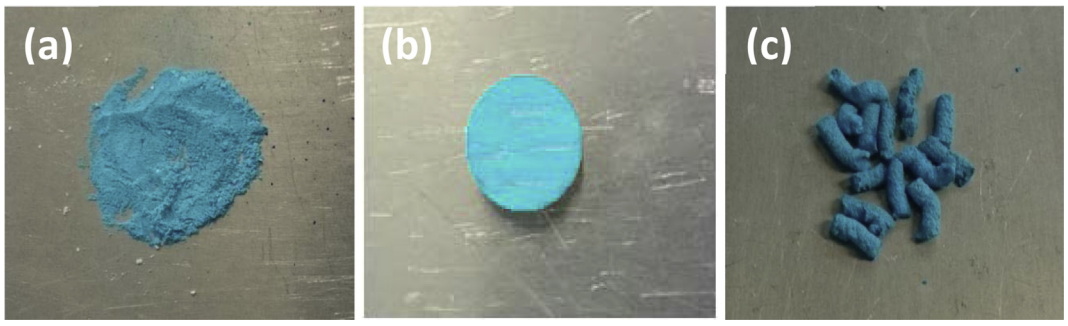

Figure 9. HKUST-1 samples: (a) powder and (b) tablet and (c) pellet.

Table 3. Surface and pore properties of HKUST-1.

HKUST-1 Sample	BET surface area m^2/g	Pore volume cc/g	Pore diameter Å
HKUST-1 powder	1271.2	0.524	14.1
HKUST-1 tablet	595.6	0.317	12.9
HKUST-1 pellet	605.1	0.124	4.26
HKUST-1 Pellet (24 h EtOH)	724.2	0.356	11.4
HKUST-1 Pellet (96 h EtOH)	896.6	0.362	12.2

For the regeneration of the MOF porous net, HKUST-1 pellets were stirred in ethanol for 24 and 96 h at room temperature. In terms of surface area, the achieved reconstruction for HKUST-1 was 74% and 92% respectively per gram of HKUST-1. The reversibility of the process was further supported by the increase in the signal intensity of the X-ray Diffraction patterns (Figure 10) after 96 h in ethanol. N_2 isotherms of the powder and the regenerated pellet (96 h in ethanol) are presented in Figure 11.

The degradation and the regeneration of the porous morphology of HKUST-1 pellets is illustrated by scanning electron microscope (SEM) images as provided in Figure 12. Primarily, the well-defined micrometer

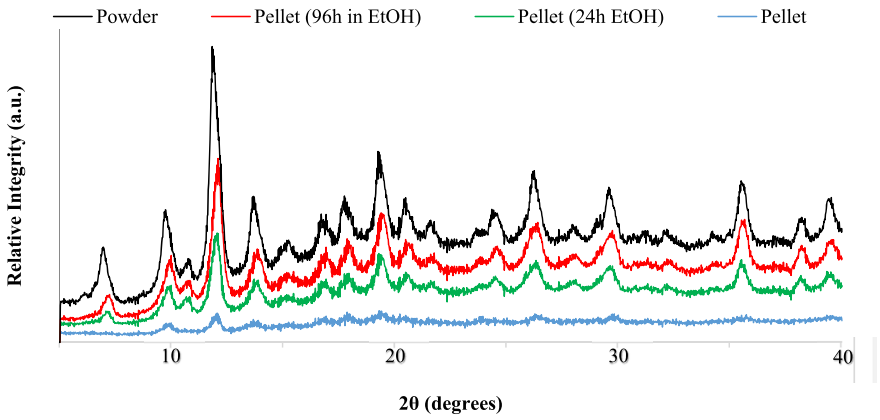

Figure 10. Comparison of the XRD patterns – HKUST-1.

sized crystals of the powder were replaced with smaller sized and less defined crystals in the case of the pellets. The size of the crystals was increased after ethanol treatment and the structure was redefined, which is in line with the XRD results. The cylindrical shaped formations that appear in the structure of both the degraded and the regenerated pellets (Figures 12b and 12c) were due to the binder and the cement that were used for the formation of the pellets.

The possible regeneration of HKUST-1 pellets was also examined based on dehydration (thermal treatment at 150 °C for 12–24 h) however the reconstruction of the porosity was unsuccessful.

3.4. Characterization of UiO-66

Similarly to HKUST-1, the morphology of UiO-66 powder was dramatically changed after the pelletization process which was reversed after ethanol treatment. Images of UiO-66 before (powder) and after pellet formation (tablet and pellet) are presented in Figure 13. BET surface area and pore volume measurements (see Table 4) indicated a 78% loss in the surface area of the pellet shaped product per gram of UiO-66, being in accordance to the lower signal intensity of the XRD patterns (Figure 14). However, the properties of the tablet were similar to the properties of the powder, proving the mechanical robustness of UiO-66. This result is in accordance with the literature [21, 30, 31, 32], where UiO-66 was found to be mechanically robust and water stable. Therefore, the collapse of its porous network may be considered not to be as a result of the applied pressure, but it is believed that the presence of the binding materials and water were the primary cause of the degradation of UiO-66.

As in the case of HKUST-1, UiO-66 pellets were stirred in ethanol for 96 h at room temperature resulting in 99.7% reconstruction of the surface area per gram of UiO-66 with a concomitant rebuilding of the crystal pores as inferred from the pore size of the treated pellets. Moreover, there

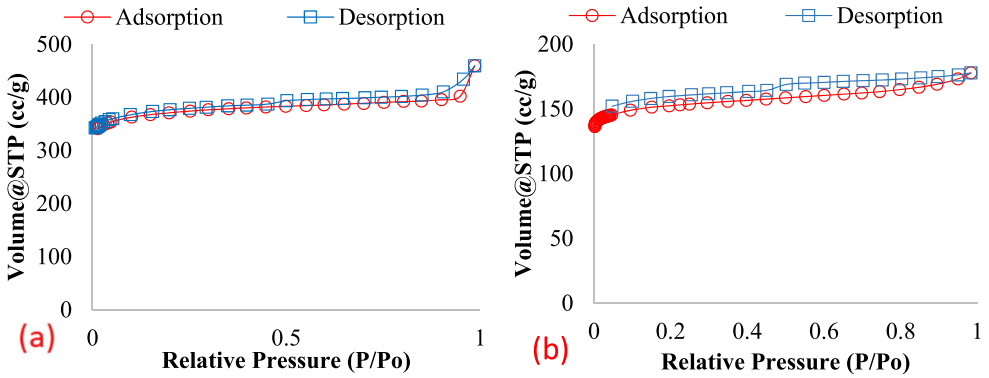

Figure 11. (a) N_2 isotherm for HKUST-1 powder (b) N_2 isotherm for HKUST-1 pellet (96 h EtOH).

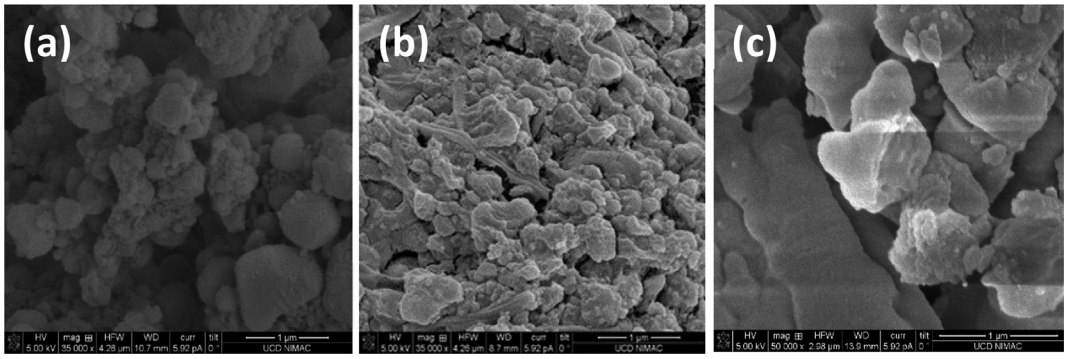

Figure 12. SEM images for HKUST-1 samples: (a) powder, (b) pellet and (c) pellet (96 h EtOH).

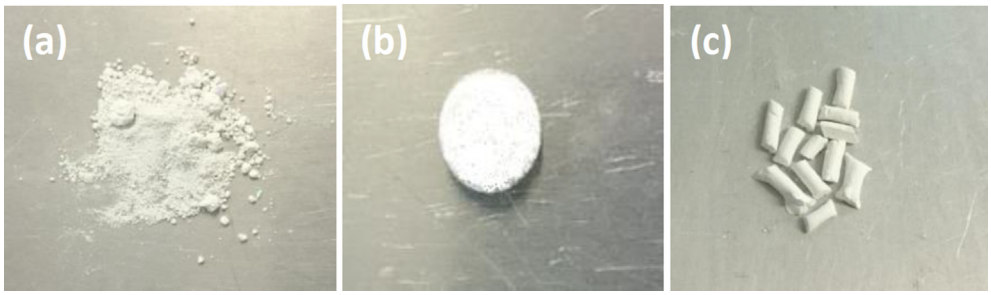

Figure 13. UiO-66 samples: (a) powder, (b) tablet and (c) pellet.

Table 4. Surface and pore properties of UiO-66.

UiO-66 Sample	BET surface area m^2/g	Pore volume cc/g	Pore Diameter Å
UiO-66 powder	1110.8	0.458	13.8
UiO-66 tablet	1095.2	0.431	13.6
UiO-66 pellet	187.4	0.329	6.4
UiO-66 pellet (96 h EtOH)	852.7	0.302	12.9

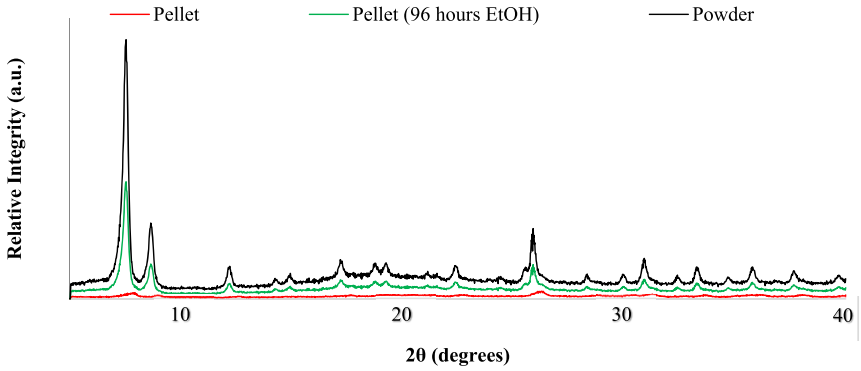

Figure 14. Comparison of the XRD patterns – UiO-66.

was a 14% decrease in the pore volume of the pellet shaped material per gram of UiO-66 (96 h EtOH) compared to the initial powder, due to the binding components. The signal intensity of the X-ray Diffraction patterns also supported the reconstruction of the crystals after ethanol treatment (Figure 14). N_2 isotherms of the powder and the regenerated pellets are presented in Figure 15.

SEM images of the three stages of UiO-66 are presented in Figure 16, showing the morphology changes of the MOF. The combination of water, binder and cement have transformed the well-shaped crystal structure of the powder into a less porous surface after pelletization. However, the presence of ethanol has rebuilt to a significant degree the crystals of the initial structure. The string formations that appear in the structure of both the degraded and the regenerated pellets (Figures 16b and 16c) were due to the binder and the cement that were used for the formation of the pellets. Finally the hardness of the UiO-66 pellets was 72.5 of Rockwell B hardness scale [33].

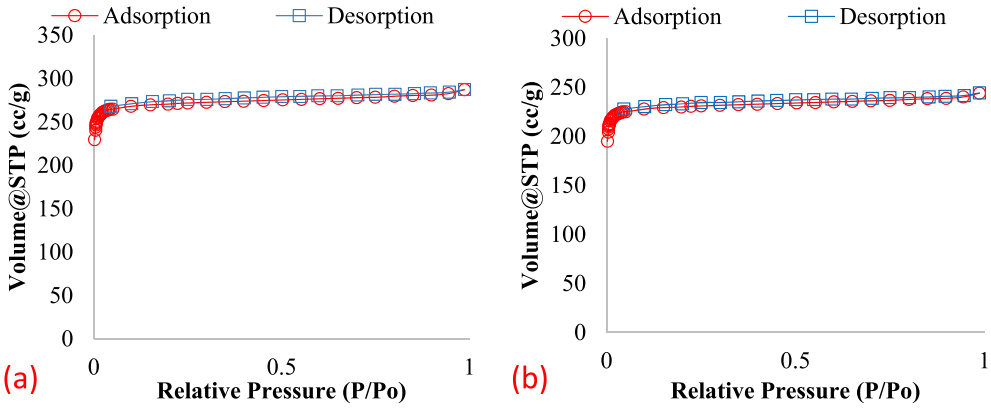

Figure 15. (a) N_2 isotherm for UiO-66 powder (b) N_2 isotherm for UiO-66 pellet.

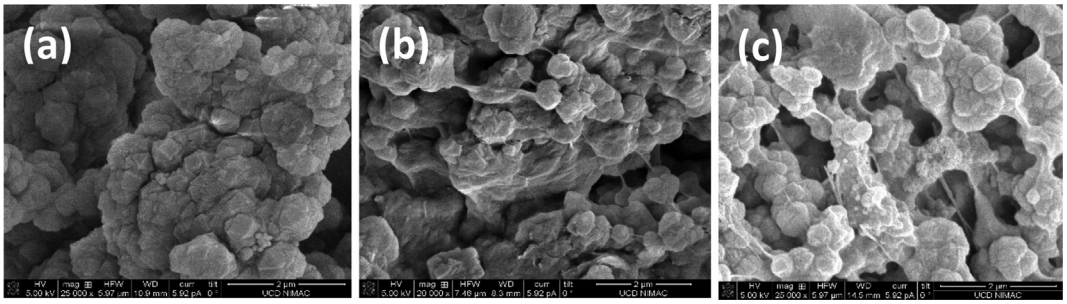

Figure 16. SEM images for UiO-66 samples: (a) powder, (b) pellet and (c) pellet (96 h EtOH).

4. Conclusions

Binder based pellets and pressure based tablets were prepared in order to examine the effects of the two pelletization processes on the physical properties of four commercial MOFs. The pellets were produced with a view to their eventual use under agitated conditions in an industrial setting and therefore commercial binders were selected in order to ensure mechanical strength. The investigation of the tablets was conducted for comparative purposes. The hardness of the pellets was similar for the four different MOFs, due to the similar amounts of additives. The structure of ZIF-8 was well maintained in the presence of binders, as well as after application of pressure. The degradation of the porous morphology of HKUST-1 in the case of the pellets was due to the presence of water and was reversible with more than 92% of the initial structure being reformed. Similarly, the surface area of UiO-66 was completely reconstructed after treatment with ethanol, with the features of the regenerated crystals within the pellet approaching those of the original powder. ZIF-67 maintained its structure in the case of pressure application (tablet), however the crystals irreversibly lost their morphological features in the presence of water and binders.

Declarations

Author contribution statement

Eleni Tsalaporta, J.M. Don MacElroy: Conceived and designed the experiments; Performed the experiments; Analyzed and interpreted the data; Contributed reagents, materials, analysis tools or data; Wrote the paper.

Funding statement

This work has been carried out as part of the Earth and Natural Sciences Doctoral Studies Programme, and was supported by the Higher Education Authority (HEA) through the Programme for Research at Third Level Institutions, Cycle 5 (PRTLI-5) and co-funded by the European Regional Development Fund (ERDF).

Competing interest statement

The authors declare no conflict of interest.

Additional information

The raw/processed data required to reproduce these findings cannot be shared at this time due to technical or time limitations.

Acknowledgements

We would like to acknowledge the assistance of Dr. K. McDonnell and Ms. S. Kerins in a number of the measurements.

References

[1] H. Li, M. Eddaoudi, M. O'Keeffe, O.M. Yaghi, Design and synthesis of an exceptionally stable and highly porous metal-organic framework, Nature (Lond.) 402 (1999) 276–279, https://doi.org/10.1038/46248.

[2] S.S.Y. Chui, S.M.F. Lo, J.P.H. Charmant, A.G. Orpen, A chemically functionalizable nanoporous material, Science 283 (1999) 1148–1150, https://doi.org/10.1126/science.283.5405.1148.

[3] K. Park, Z. Ni, A. Cote, J. Choi, R. Huang, F. Uribe-Romo, H. Chae, M. O'Keeffe, O. Yaghi, Exceptional chemical and thermal stability of zeolitic imidazolate frameworks, Proc. Natl. Acad. Sci. Unit. States Am. 103 (2006) 10186–10191, https://doi.org/10.1073/pnas.0602439103.

[4] N.A. Khan, I.J. Kang, H.Y. Seok, S.H. Jhung, Facile synthesis of nano-sized metal-organic frameworks, chromium-benzenedicarboxylate, MIL-101, Chem. Eng. J. 166 (2011) 1152–1157, https://doi.org/10.1016/j.cej.2010.11.098.

[5] A.E. Martinez Joaristi, J. Juan Alcaniz, J.P. Serra Crespo, F. Kapteijn, J. Gascon, Electrochemical synthesis of some archetypical Zn^{2+}, Cu^{2+}, and Al^{3+} metal organic frameworks, Cryst. Growth Des. 12 (2012) 3489–3498, https://doi.org/10.1021/cg300552w.

[6] N. Stock, S. Biswas, Synthesis of metal-organic frameworks (MOFs): routes to various MOF topologies, morphologies, and composites, Chem. Rev. 112 (2012) 933–969, https://doi.org/10.1021/cr200304e.

[7] R. Sabouni, H. Kazemian, S. Rohani, Carbon dioxide adsorption in microwave-synthesized metal organic framework CPM-5: Equilibrium and kinetics study, Microporous Mesoporous Mater. 175 (2013) 85–91, https://doi.org/10.1016/j.micromeso.2013.03.024.

[8] Y. Lee, J. Kim, W. Ahn, Synthesis of metal-organic frameworks: A mini review, Kor. J. Chem. Eng. 30 (2013) 1667–1680, https://doi.org/10.1007/s11814-013-0140-6.

[9] M. Eddaoudi, J. Kim, N. Rosi, D. Vodak, J. Wachter, M. O'Keeffe, O.M. Yaghi, Systematic design of pore size and functionality in isoreticular MOFs and their application in methane storage, Science 295 (2002) 469–472, https://doi.org/10.1126/science.1067208.

[10] A.R. Millward, O.M. Yaghi, Metal−organic frameworks with exceptionally high capacity for storage of carbon dioxide at room temperature, J. Am. Chem. Soc. 127 (2005) 17998–17999, https://doi.org/10.1021/ja0570032.

[11] J. Liu, Y. Wang, A. Benin, P. Jakubczak, R. Willis, M. LeVan, CO_2/H_2O adsorption equilibrium and rates on metal−organic frameworks: HKUST-1 and Ni/DOBDC, Langmuir 26 (2010) 14301–14307, https://doi.org/10.1021/la102359q.

[12] D. Liu, Y. Wu, Q. Xia, Z. Li, H. Xi, Experimental and molecular simulation studies of CO_2 adsorption on zeolitic imidazolate frameworks: ZIF-8 and amine-modified ZIF-8, Adsorption 19 (2012) 25–37, https://doi.org/10.1007/s10450-012-9407-1.

[13] M. De Toni, R. Jonchiere, P. Pullumbi, F. Coudert, A. Fuchs, How can a hydrophobic MOF be water-unstable? Insight into the hydration mechanism of IRMOFs, ChemPhysChem 13 (2012) 3497–3503, https://doi.org/10.1002/cphc.201200455.

[14] P.M. Schoenecker, C.G. Carson, H. Jasuja, C.J.J. Flemming, K.S. Walton, Effect of water adsorption on retention of structure and surface area of metal–organic frameworks, Ind. Eng. Chem. Res. 51 (2012) 6513–6519, https://doi.org/10.1021/ie202325p.

[15] J. Liu, P.K. Thallapally, B.P. McGrail, D.R. Brown, J. Liu, Progress in adsorption-based CO_2 capture by metal–organic frameworks, Chem. Soc. Rev. 41 (2012) 2308–2322.

[16] K. Sumida, D.L. Rogow, J.A. Mason, T.M. McDonald, E.D. Bloch, Z.R. Herm, T.H. Bae, J.R. Long, Carbon dioxide capture in metal–organic frameworks, Chem. Rev. 112 (2012) 724–781, https://doi.org/10.1021/cr2003272.

[17] J. McEwen, J. Hayman, A. Ozgur Yazaydin, A comparative study of CO_2, CH_4 and N_2 adsorption in ZIF-8, Zeolite-13X and BPL activated carbon, Chem. Phys. 412 (2013) 72–76, https://doi.org/10.1016/j.chemphys.2012.12.012.

[18] Z. Zhang, Y. Zhao, Q. Gong, Z. Li, J. Li, MOFs for CO_2 capture and separation from flue gas mixtures: the effect of multifunctional sites on their adsorption capacity and selectivity, Chem. Commun. 49 (2013) 653–661.

[19] M. Alhamami, H. Doan, C. Cheng, A review on breathing behaviors of metal-organic-frameworks (MOFs) for gas adsorption, Materials 7 (2014) 3198–3250, https://doi.org/10.3390/ma7043198.

[20] B. Xiao, P.S. Wheatley, X. Zhao, A.J. Fletcher, S. Fox, A.G. Rossi, I.L. Megson, S. Bordiga, L. Regli, K.M. Thomas, R.E. Morris, High-capacity hydrogen and nitric oxide adsorption and storage in a metal-organic framework, J. Am. Chem. Soc. 129 (2007) 1203–1209, https://doi.org/10.1021/ja066098k.

[21] G.W. Peterson, J.B. DeCoste, T. Grant Glover, Y. Huang, H. Jasuja, K.S. Walton, Effects of pelletization pressure on the physical and chemical properties of the metal–organic frameworks Cu3(BTC)2 and UiO-66, Microporous Mesoporous Mater. 179 (2013) 48–53.

[22] V. Finsy, L. Ma, L. Alaerts, D.E. De Vos, G.V. Baron, J.F.M. Denayer, Separation of CO_2/CH_4 mixtures with the MIL-53(Al) metal–organic framework, Microporous Mesoporous Mater. 120 (2009) 221–227, https://doi.org/10.1016/j.micromeso.2008.11.007.

[23] L.D. O'Neill, H. Zhang, D. Bradshaw, Macro-/microporous MOF composite beads, J. Mater. Chem. 20 (2010) 5720–5726.

[24] J.A. Delgado, V.I. Águeda, M.A. Uguina, P. Brea, C.A. Grande, Comparison and evaluation of agglomerated MOFs in biohydrogen purification by means of pressure swing adsorption (PSA), Chem. Eng. J. 326 (2017) 117–129, https://doi.org/10.1016/j.cej.2017.05.144.

[25] S. Edubilli, S. Gumma, A systematic evaluation of UiO-66 metal organic framework for CO_2/N_2 separation, Separ. Purif. Technol. 224 (2019) 85–94, https://doi.org/10.1016/j.seppur.2019.04.081.

[26] D.W. Lee, T. Didriksen, U. Olsbye, R. Blom, C.A. Grande, Shaping of metal-organic framework UiO-66 using alginates: effect of operation variables, Separ. Purif. Technol. 235 (2020), https://doi.org/10.1016/j.seppur.2019.116182.

[27] E. Tsalaporta, N. Brady, J.M.D. MacElroy, Experimental and modelling studies of CO_2/N_2 mixture separations using amine functionalised silicas, Adsorption 23 (2017) 847–869, https://doi.org/10.1007/s10450-017-9896-z.

[28] K. Mathivathani, M.H. Nilsen, S. Usseglio, S. Jakobsen, U. Olsbye, M. Tilset, C. Larabi, E.A. Quadrelli, F. Bonino, K.P. Lillerud, Synthesis and stability of tagged UiO-66 Zr-MOFs, Chem. Mater. 22 (24) (2010) 6632–6640, https://doi.org/10.1021/cm102601v.

[29] G. Majano, O. Martin, M. Hammes, S. Smeets, C. Baerlocher, J. Pérez-Ramírez, Solvent-mediated reconstruction of the metal–organic framework HKUST-1 ($Cu_3(BTC)_2$), Adv. Funct. Mater. 24 (2014) 3855–3865, https://doi.org/10.1002/adfm.201303678.

[30] J. Cavka, S. Jakobsen, U. Olsbye, N. Guillou, C. Lamberti, S. Bordiga, K.J. Lillerud, A new zirconium inorganic building brick forming metal organic frameworks with exceptional stability, Am. Chem. Soc. 130 (42) (2008) 13850–13851, https://doi.org/10.1021/ja8057953.

[31] J. Hafizovic, S. Jakobsen, U. Olsbye, N. Guillou, C. Lamberti, S. Bordiga, K.P. Lillerud, A new zirconium inorganic building brick forming metal organic frameworks with exceptional stability, J. Am. Chem. Soc. 130 (2008) 13850–13851, https://doi.org/10.1021/ja8057953.

[32] J.B. DeCoste, G.W. Peterson, B.J. Schindler, K.L. Killops, M.A. Broweb, J.J. Mahleb, The effect of water adsorption on the structure of the carboxylate containing metal–organic frameworks Cu-BTC, Mg-MOF-74, and UiO-66, J. Mater. Chem. 1 (2013) 11922–11932.

[33] E. Tsalaporta, S. Vaesen, J.M.D. MacElroy and W. Schmidtt, *Adsorbent Media*, Patent: TCD Tech ID WS01-759-01,UK IPO